Comparison of experimental and theoretical integral cross sections for $D+H_2(v=1,j=1)\rightarrow HD(v'=1,j')+H$

Dahv A. V. Kliner,[a] David E. Adelman, and Richard N. Zare
Department of Chemistry, Stanford University, Stanford, California 94305

(Received 18 March 1991; accepted 23 April 1991)

We have measured the nascent $HD(v'=1,j')$ product rotational distribution from the reaction $D+H_2(v,j)$ in which the H_2 reagent was either thermal $(v=0,j)$ or prepared in the level $(v=1,j=1)$ by stimulated Raman pumping. Translationally hot D atoms were obtained by uv laser photolysis of DBr or DI. Photolysis of DBr generated D atoms with center-of-mass collision energies (E_{rel}) of 1.04 and 0.82 eV, which corresponded to the production of ground state Br and spin–orbit-excited Br*, respectively. The E_{rel} values for DI photolysis were 1.38 and 0.92 eV. Quantum-state-specific detection of HD was accomplished via (2 + 1) resonance-enhanced multiphoton ionization and time-of-flight mass spectrometry. Vibrational excitation of the H_2 reagent results in substantial rotational excitation of the $HD(v'=1)$ product and increases the reaction rate into $v'=1$ by about a factor of 4. Although the quantum-mechanical calculation of Blais *et al.* [Chem. Phys. Lett. **166**, 11 (1990)] for the $D+H_2(v=1,j=1)\rightarrow HD(v'=1,j')+H$ product rotational distribution at $E_{rel}=1.02$ eV is in qualitative agreement with experiment, it does not quantitatively agree with the measured distribution. Specifically, the calculated distribution is too hot by 2–3 rotational quanta, and the predicted enhancement in the $v'=1$ rate with reagent vibrational excitation is too large by $67\% \pm 9\%$.

I. INTRODUCTION

A common misconception of how science is done is that it follows a self-corrective approach of gathering data, formulating hypotheses, testing models, and making laws.[1,2] Of course, the interplay between theory and experiment is actually much more involved. In chemistry, observations are seldom compared with theoretical predictions based on first principles because chemistry concerns phenomena that are too complex. An outstanding exception is the electronic structure and static properties of small molecules composed of atoms in the first few rows of the periodic table. For such molecules *ab initio* quantum calculations are "sufficiently accurate to complement experiment and to yield considerable insight into the nature of the bonding."[3] For elementary chemical reactions, however, the $H+H_2\rightarrow H_2+H$ reaction and its isotopic variants is the only system for which fully converged, three-dimensional, quantum-mechanical scattering calculations have been performed on a "chemically accurate," *ab initio* potential energy surface (PES).[4–12] Hereafter, we refer to computations of this quality as "QM calculations." In this paper, we report measurements of the $HD(v'=1,j')$ rotational distribution for the reaction $D+H_2(v=1,j=1)$ and compare them with the best available QM calculation.[5] Significant differences are found. We do not attempt to reconcile theory and experiment. Instead, emphasis is placed on the experimental results and the checks performed to ensure their validity.

In the past few years, advances in reactive scattering algorithmic methods have made possible QM calculations for the $H+H_2$ reaction and its isotopic variants over a wide range of initial conditions.[4–12] Parallel developments in experimental methodologies involving laser and molecular-beam techniques have provided measurements[13–24] that are being used to test these benchmark theoretical calculations. In the short time since $H+H_2$ QM calculations have become available, they have been compared with the experimental results of several groups for the reactions $H+$*para*-H_2,[23] $H+D_2$,[11] and $D+H_2$.[5,8,17,19,22] Experimental and theoretical results have been in generally good agreement, but some outstanding differences have been noted.

QM theory and experiment are in close agreement for the total reaction cross section at a given collision energy in both cases for which comparison is possible. For the $H+D_2(v=0)$ reaction at $E_{rel}=1.3$ eV, the calculated cross section of D'Mello, Manolopoulos, and Wyatt[11] (1.06 Å^2) agrees well with the measurements of Levene *et al.*[14] (1.1 ± 0.4 Å^2) and of Johnston *et al.*[15] (1.13 ± 0.17 Å^2, obtained by interpolation of measurements at other energies). Similar agreement was obtained when the H_2 reagent was vibrationally excited. Zhang and Miller's[8] calculated cross section of 1.47 Å^2 for the reaction $D+H_2(v=1,j=0)$ at $E_{rel}=0.33$ eV agrees within experimental uncertainty with the value of 1.14 ± 0.50 Å^2 measured by Götting *et al.*[16]

Two groups have measured product-state-resolved, integral cross sections for isotopic variants of the $H+H_2$ reaction at several collision energies. In the few cases for which comparisons have been made, QM calculations nearly perfectly reproduce the experimental results when the reagent is in the ground vibrational state. In particular, there is excellent agreement between QM theory and experiment for the reactions $H+$*para*-$H_2\rightarrow H_2(v'=1,j')+H$ at $E_{rel}=0.83$–1.00 eV,[7,23] $H+D_2\rightarrow HD(v',j')+H$ at $E_{rel}=1.3$ and 0.55 eV,[11,13,20] and $D+H_2\rightarrow HD(v'=1,j')+H$ at $E_{rel}=1.0$ eV.[6,8,22]

As noted by Buntin, Giese, and Gentry,[18] "...the differential cross sections for this reaction are considerably more

[a] Present address: Department of Chemistry, University of Minnesota, Minneapolis, Minnesota 55455.

 0021-9606/91/151648-15$03.00

sensitive to the details of the potential energy surface and/or the dynamics than are the integral cross sections." To date, no experiment that fully resolves both product angular and internal-state distributions has been performed, although indications are that such experiments will be possible in the future.[25] Two groups have succeeded, however, in measuring $D + H_2$ differential (angle-resolved) cross sections with partial internal state resolution by crossed-beam experiments. Buntin, Giese, and Gentry[17,18] measured HD time-of-flight (TOF) distributions at a fixed laboratory scattering angle for six values of E_{rel} between 0.85 and 1.20 eV. Continetti, Balko, and Lee[19] recorded HD TOF distributions at many scattering angles for $E_{rel} = 0.53$ and 1.01 eV. After averaging the QM results of Zhang and Miller[8] and of Zhao *et al.*[6] over their respective experimental resolution functions, both experimental groups found overall good agreement between QM theory and experiment. Differences were noted, however, between the calculated and measured TOF distributions. These workers speculated that these discrepancies are caused by errors in the H_3 PESs used in the computations, with emphasis on possible errors in the calculated bend potentials.[18,19]

A possible exception to the excellent agreement between QM and experimental integral cross sections was recently reported for a vibrationally excited reagent. Kliner and Zare (KZ) (Ref. 21) measured the nascent product rotational distribution for the reaction $D + H_2(v=1, j=1) \rightarrow HD(v'=1, j') + H$ at $E_{rel} = 1.0$ eV, in which photolysis of DBr generated translationally hot D atoms. The H_2 reagent was prepared in the level ($v = 1$, $j = 1$) by stimulated Raman pumping (SRP), and quantum-state-specific detection of the molecular reaction product was accomplished via (2 + 1) resonance-enhanced multiphoton ionization (REMPI) (Ref. 26) and time-of-flight mass spectrometry (TOF/MS). KZ found that vibrational excitation of the H_2 reagent results in substantial rotational excitation of the $HD(v' = 1)$ product and increases the reaction rate into $v' = 1$ by at least a factor of 4.

Subsequently, Blais, Zhao, Truhlar, Schwenke, and Kouri (BZTSK) (Ref. 5) performed a QM scattering calculation on the DMBE surface[27] to simulate this experiment and found qualitatively good agreement. However, in contrast to the situation for which the H_2 reagent was in $v = 0$,[22] the shapes of the measured and QM distributions were not in quantitative agreement.[5] The QM distribution was rotationally hotter than that obtained from the experiment, and the calculated increase in the $v' = 1$ rate upon reagent vibrational excitation was larger than the measured value. The significance of these differences could not be assessed because of two limitations in the previous experiment. First, a relatively small fraction (13%) of the H_2 was promoted into $v = 1$. Since reaction occurred with both the $v = 0$ and $v = 1$ reagents, the $v = 0$ contribution (87% of all reagents) had to be subtracted from the measured distribution; this subtraction resulted in relatively large experimental uncertainties. Second, the subtraction procedure contained the (untested) assumption that integral cross sections for the reaction $D + H_2(v=0, j) \rightarrow HD(v'=1, j') + H$ have no dependence on j.

In this paper we report new measurements for the reaction $D + H_2(v,j) \rightarrow HD(v',j') + H$ at $E_{rel} = 1.0$ and 1.4 eV. Experimental improvements have minimized the two limitations discussed above. The SRP efficiency was increased so that 34% of the H_2 was pumped into ($v = 1, j = 1$), which allowed the $D + H_2(v=1, j=1) \rightarrow HD(v'=1, j') + H$ state-to-state rotational distribution to be determined more accurately. The validity of the assumption used in analyzing the data was tested by comparing $HD(v'=1, j')$ product rotational distributions for the reactions $D + normal\text{-}H_2$ and $D + para\text{-}H_2$. Several additional experimental checks were performed, including comparable experiments using photolysis of DI rather than DBr. The differences persist between the experimental and theoretical results at $E_{rel} = 1.0$ eV. Specifically, the calculated rotational distribution is 2–3 quanta hotter than that obtained from the experiment, and the predicted enhancement in the $v' = 1$ rate that occurs upon reagent vibrational excitation is too large by 67%.

II. EXPERIMENT

A. Overview

An overview of the experimental setup is shown in Fig. 1 and the vacuum chamber is detailed in Fig. 2. DX (X = Br or I, Cambridge Isotope Labs, 99% D stated isotopic abundance) was purified by a freeze–pump–thaw cycle and mixed with H_2 (Linde, 99.9995 + % stated purity) and He (Linde, 99.999% stated purity) in the ratio $DX:H_2:He = 1:3:15–20$. The reagents flowed via a pulsed nozzle into a high vacuum chamber. This vertical reagent beam was crossed by the focused, copropagating SRP beams ($\lambda = 532$ and 683 nm). After a delay of 15–20 ns, a second laser ($\lambda \approx 210$ nm) was fired to photodissociate the DX, yielding fast D atoms. This laser pulse also ionized the HD reaction product via (2 + 1) REMPI (Ref. 26). Because the same laser pulse effected both photolysis and detection, the observed reaction products represent those formed within the pulse duration (~ 5 ns). The photolysis/probe laser consisted of a 10 Hz, Nd:YAG-pumped dye laser (Spectra-Physics, DCR-3G, PDL-1) with frequency-doubling and mixing stages (INRAD Autotracker II, β-barium borate crystals[29]). The HD^+ ions were detected in a shuttered TOF/MS.[30]

The REMPI-TOF/MS detection procedure has been calibrated against a high-temperature, effusive nozzle source of HD, thereby allowing the measured ion signals to be related to relative quantum-state populations[26] Because the integrated area of a REMPI spectral peak corresponds to the density of that quantum state, the measured product rotational distributions correspond to the relative rates of reaction into those states.[20] These rate constants are related to (average) cross sections via multiplication by the relative velocity of the reagents.[31]

The experimental apparatus and procedure were the same as those described previously[20,23,30] with two modifications: (1) the continuous, effusive, capillary nozzle used in earlier studies was replaced with a pulsed, supersonic nozzle, and (2) the SRP Nd:YAG laser used in the preliminary

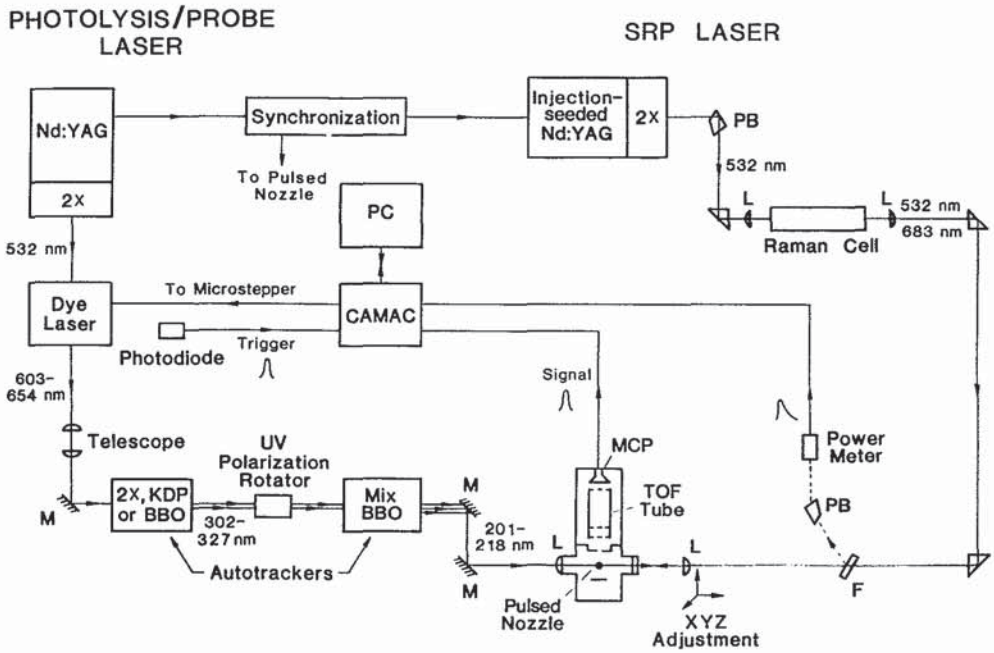

FIG. 1. Schematic diagram of the experiment configuration. M = dichroic mirror, L = lens, PB = Pellin–Broca prism, F = BK-7 flat, MCP = multichannel-plate detector, and PC = personal computer.

experiment of KZ was replaced with a higher-power, injection-seeded laser. These modifications and the experimental checks and characterization studies are described below.

B. Pulsed-nozzle characterization

In our previous studies of the $H+H_2$ reaction family,[20–23,28,30] the reagents flowed effusively and continuously into the vacuum chamber via a quartz capillary nozzle. Under such "bulb" conditions, the spread in the translational energy distribution arising from thermal motions of the reagents is large.[32] For the $D+H_2$ reaction at $E_{rel}=1.06$ eV, in which fast D atoms are generated by DBr photolysis at 210 nm, the E_{rel} distribution at 300 K is nearly Gaussian with a FWHM of 0.39 eV. The width of this distribution scales as $T^{1/2}$, where T is the translational temperature in Kelvin. A pulsed nozzle (General Valve Series 9, 0.76 mm orifice diameter) was incorporated into the apparatus to improve the experimental energy resolution by narrowing the reagent translational energy distribution. As discussed below, we estimate that incorporation of the pulsed nozzle reduced the spread in E_{rel} by a factor of 5.

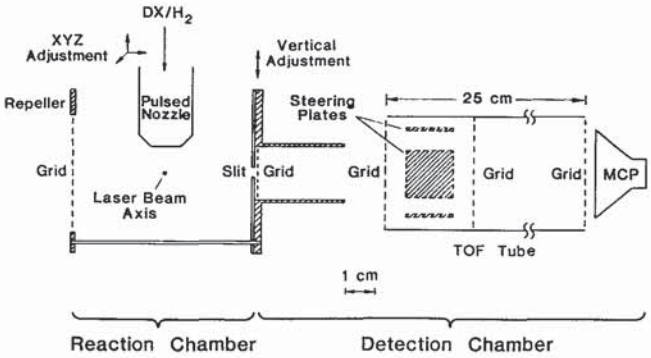

FIG. 2. Expanded view of the reaction and detection chambers.

Several checks were performed to ensure that the REMPI ion signal still arose from the nascent reaction product and to characterize the performance of the nozzle. In particular, we investigated collisional relaxation of the reagents and reaction products and checked for clustering in the expansion. We measured rotational distributions of

(1) the $H_2(v'=1)$ product of the H + HI reaction using neat HI and HI seeded in He as a function of seeding ratio, nozzle backing pressure, and distance between the nozzle orifice and the laser beams, which we refer to as the "nozzle height;"
(2) the $HD(v'=1)$ product of the $H+D_2$ reaction as a function of nozzle backing pressure and $HI:D_2:He$ mix ratio;
(3) the $HD(v'=1)$ product of the $H+D_2$ reaction as a function of delay between the photolysis and probe lasers; and
(4) $H_2(v=0)$ and $D_2(v=0)$ diluted in He as a function of time within the nozzle pulse.

In studies (1)–(3), separate lasers were used for photolysis of HI ($\lambda=266$ nm) and for REMPI detection of molecular hydrogen ($\lambda=208$–218 nm). The photolysis pulse was provided by a frequency-quadrupled Nd:YAG laser (10 Hz; Spectra-Physics, DCR-1A or injection-seeded GCR-4). Photolysis of HI at 266 nm generated translationally hot H atoms with $E_{rel}=1.3$ and 0.55 eV for the $H+D_2$ reaction (1.61 and 0.67 eV for H + HI) in the ratio 64:36, corresponding to the production of ground state $I(^2P_{3/2})$ and spin–orbit-excited $I(^2P_{1/2})$, respectively.[33]

The results of these pulsed-nozzle characterization studies were as follows:

(1) No variation was observed in the $H_2(v'=1,j')$ product rotational distribution for the H + HI reaction for HI:He ratios between 1:0 and 1:47, nozzle backing pressures between 30 and 550 Torr, and nozzle heights of 4 to 9 mm.

Moreover, the measured distributions were in good agreement with the $H_2(v'=1,j')$ distribution obtained previously with the capillary nozzle.[34] These observations suggest that either there was no significant clustering of the HI under our experimental conditions or such clustering did not substantially perturb the translation energy distribution of the H-atom reagent.

(2) From measurements of the $HD(v'=1)$ product of the $H+D_2$ reaction at $E_{rel}=1.3$ and 0.55 eV, we determined that the optimum conditions for operation of the pulsed nozzle were a backing pressure of 500 Torr, a nozzle height of 9 mm (12 nozzle diam), and a nozzle pulse width of $\sim 600\,\mu$s. No variation in the $HD(v'=1,j')$ product rotational distribution was observed for $HI:D_2$ mix ratios between 1:1 and 1:8, $(HI+D_2)$:He ratios between 1:0 and 1:6, and nozzle backing pressures between 350 and 550 Torr. Most of these studies were performed with a 9 mm nozzle height and with a delay of 60 ns between the photolysis- and probe-laser pulses, the same delay as used in previous studies with the capillary nozzle[20] [see also point (3) below]. Figure 3 displays a comparison of $HD(v'=1,j')$ product rotational distributions measured with the capillary and pulsed nozzles. The excellent agreement between these distributions again indicates that the use of the pulsed nozzle did not introduce systematic errors.

(3) In the course of our previous measurements on the $H+D_2$ reaction, the $HD(v'=1,j')$ product rotational distribution was measured as a function of delay time between the photolysis- and probe-laser pulses to check for product relaxation or flyout from the detection volume.[20] No change occurred in this distribution for delays of less than 110 ns. We performed similar measurements with the pulsed nozzle (9 mm nozzle height, 500 Torr backing pressure, 1:9:50 $HI:D_2$:He ratio) and found no change in the distributions for delay times between 35 and 135 ns. For the $D+H_2$ experiments reported here, initiation and probing of the reaction occurred within a single laser pulse of ~ 5 ns duration.[28] Thus, we were well within the single-collision regime.

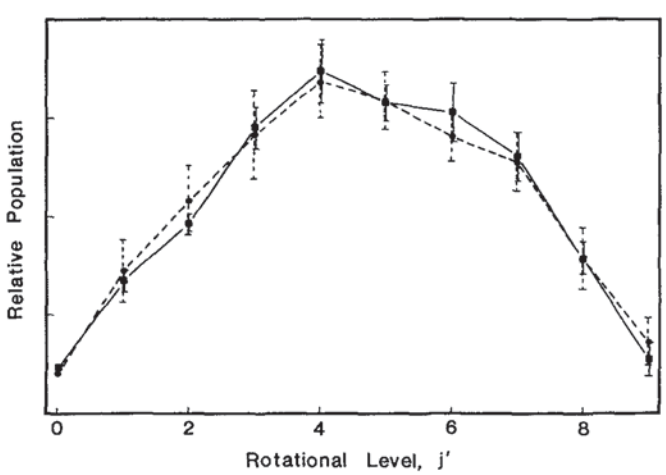

FIG. 3. Comparison of the $HD(v'=1,j')$ product rotational distributions obtained with the pulsed nozzle (squares connected by solid lines) and with the effusive nozzle (circles connected by dashed lines; Ref. 20) from the reaction $H+D_2$ at $E_{rel}=1.3$ and 0.55 eV. Error bars represent one standard deviation.

(4) The rotational distributions of dilute ($\sim 10^{-5}\%$) H_2 and D_2 in He were measured to study relaxation in the expansion as a function of time within the nozzle pulse (500 Torr backing pressure, 9 mm nozzle height). For $D_2(v=0, j=0\text{–}4)$, curvature was found for Boltzmann plots of $\ln[P(j)/(2j+1)g_j]$ vs $E(j)$, where $P(j)$ is the population of the level $(v=0,j)$, $E(j)$ is the rotational energy of that level, and g_j is the nuclear spin degeneracy.[35] Such curvature is typical for partially relaxed hydrogen.[26,36] For the lowest three rotational levels of $D_2(v=0)$, which contain 95% of the population, the Boltzmann plots were straight and yielded rotational temperatures of ~ 100 K within $\pm 100\,\mu$s of the center of the nozzle pulse. For times closer to the beginning or end of the nozzle pulse, the temperatures were hotter (~ 140 K). For $H_2(v=0,j=0\text{–}3)$, the Boltzmann plot was straight and yielded a rotational temperature of 150 K. The latter measurement is expected to provide a good estimate of the reagent rotational temperature in the studies of the $D+H_2$ reaction since He was the major component in both cases ($\sim 80\%$ He in the reactive studies).

As mentioned above, the primary purpose of incorporating the pulsed nozzle into the apparatus was to obtain a narrower collision energy distribution. Although this distribution could not be measured directly with our apparatus, it can be estimated with knowledge of the nozzle conditions. Additionally, the measurements of $H_2(v=0)$ and $D_2(v=0)$ rotational distributions [point (4) above] put an upper bound on the translational temperature, since rotational relaxation of molecular hydrogen requires significantly more collisions than does translational relaxation (the rotational collision number of H_2 is ~ 300, whereas the translational collision number is 1).[37] With a backing pressure of 500 Torr and nozzle diameter of 0.76 mm, continuum flow is expected to occur for most or all of the 9 mm between the nozzle orifice and the laser beams. For pure He initially at 293 K, the experimental measurements and theoretical calculations of Toennies and co-workers[38] predict a translational temperature of ~ 1 K. For our mixture of He, H_2, and DX, velocity slip probably increased the effective translational temperature.[37] At 10 K, for example, the spread in translational energy for the $D+H_2$ reaction at $E_{rel}=1.0$ eV is 0.07 eV FWHM,[32] an improvement in energy resolution of a factor of 5 with respect to the effusive nozzle. Note that this value represents an estimate, not a measurement under our experimental conditions.

C. Stimulated Raman pumping

Stimulated Raman pumping allows the preparation of a single rovibrational level in the ground electronic state of a molecule (see Ref. 21 for references to other experiments employing SRP). SRP requires two laser beams with a frequency difference that matches a Raman-allowed transition, $H_2(v=0,j=1)\rightarrow H_2(v=1,j=1)$ in the present experiment. In the preliminary studies of the $D+H_2(v=1, j=1)$ reaction,[21] 19% of the $H_2(v=0,j=1)$ population, which corresponded to 13% of the total population, was

pumped into $(v=1, j=1)$ [at 294 K, $H_2(v=0, j=1)$ contains 66% of the total population].

The SRP laser used by KZ was replaced with a higher-power, injection-seeded Nd:YAG laser (Spectra-Physics, GCR-4), which allowed the SRP transition to be saturated, i.e., 50% of the $H_2(v=0, j=1)$ population was promoted into $H_2(v=1, j=1)$. In addition, the SRP shot-to-shot stability was improved. The wavelengths of the SRP beams were 532 nm (second harmonic of the Nd:YAG laser) and 683 nm (first Stokes from the 532 nm beam passing through an H_2 Raman cell, 29 psig); see Fig. 1. The 532 nm beam was focused into the Raman cell with a 500 mm f. l. lens, and the emerging beams were recollimated with a 350 mm f. l. lens. The output of the Raman cell was passed through a BK-7 flat to remove the uv anti-Stokes orders that could photolyze DX; this flat also provided a backreflection of the counterpropagating ~210 nm photolysis/probe beam used for power normalization. Typical pulse energies were 25 mJ each in the 532 and 683 nm beams.

The SRP beams were focused into the chamber by a quartz lens (Esco, Suprasil B, 200 mm f. l.) mounted on an x–y–z translation stage, thereby allowing optimization of their overlap with the counterpropagating photolysis/probe beam, which was also focused by a quartz lens (Esco, Suprasil B, 125 mm f. l.). The 200 mm f. l. lens also collimated the photolysis/probe beam as it emerged from the vacuum chamber.

The SRP efficiency is defined as

$$1-\frac{[H_2(v=0,j=1)\text{ with SRP}]}{[H_2(v=0,j=1)\text{ without SRP}]}, \qquad (1)$$

where $[\cdots]$ denotes density. The SRP efficiency was measured by recording $H_2(v=0, j=1)$ REMPI spectra both with and without Raman pumping, as shown in Fig. 4. The reduction in the area under the peak in the presence of the SRP beams [Fig. 4(a)] represents the fraction of the population excited into $(v=1, j=1)$. Figure 4(b) shows that upon doubling the spectral peak recorded with SRP, the peaks recorded with and without SRP are the same size, demonstrating saturation of the SRP transition (50% efficiency). As verified by REMPI, SRP did not populate $j\neq 1$ levels of $H_2(v=1)$. Because of rotational cooling in the supersonic expansion [Sec. II B, point (4)], the initial population of $H_2(v=0, j=1)$ was 71% in the present experiment. Thus, a Raman pumping efficiency of 50% corresponds to promotion of 35.5% of the H_2 into $v=1$.

D. DX photolysis

1. E_{rel} and X*/X values

Ultraviolet laser photolysis of DX (X = Br or I) was used to generate translationally hot D atoms for the reactive studies. Because DX was photolyzed by the tunable probe laser ($\lambda = 208$–218 nm), the photolysis wavelength and therefore E_{rel} was varied as different $HD(v'=1, j')$ rotational levels were detected. The variation in E_{rel} with j' is approximately equal to the estimated thermal spread in E_{rel} (~0.07 eV, Sec. II B) and represents only a minor complication. Another consideration in the photolysis of DX is the production of two groups of D atoms with different speeds

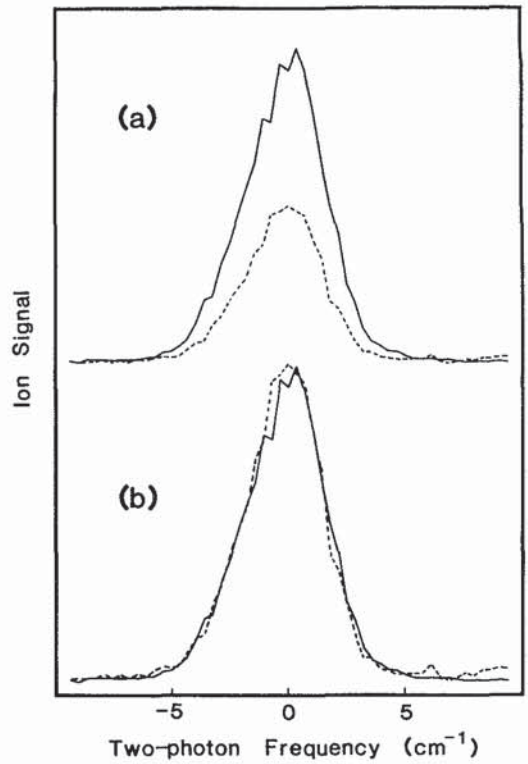

FIG. 4. (a) $H_2(v=0, j=1)$ REMPI spectral peaks without SRP (solid curve) and with SRP (dashed curve). (b) Same as (a), but with the dashed curve multiplied by 2. On the abscissa, 0 denotes line center.

that correspond to the production of ground state $X(^2P_{1/2})\equiv X$ and spin–orbit-excited $X(^2P_{1/2})\equiv X^*$. Figure 5 shows E_{rel} values as a function of j' for the $D+H_2$ reaction for both the X and X* channels in the photolysis of DBr and DI. Although the variation in E_{rel} with j' is relatively minor, the difference in E_{rel} between the X and X* photolysis channels is substantial. Therefore, DX photolysis produces a bimodal distribution of collision energies. For DBr at the present photolysis wavelengths, the peaks of this distribution are at 1.04 and 0.82 eV; for DI, these two collision energies are

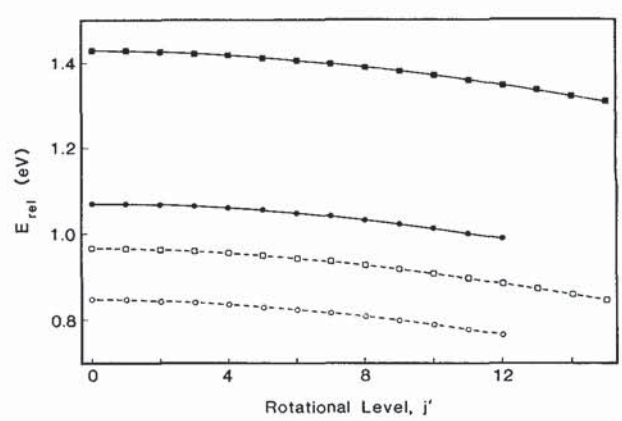

FIG. 5. Center-of-mass collision energy as a function of rotational quantum number for the reaction $D+H_2\rightarrow HD(v'=1,j')+H$, where D atoms are generated by photolysis of DX (squares for X = I, circles for X = Br). The solid symbols connected by solid lines denote the DX photolysis channel that produces ground state X atoms; the open symbols connected by dashed lines denote the X* channel.

1.38 and 0.92 eV. For convenience, we will often refer to the experiment using DBr (DI) photolysis as having a collision energy of 1.0 (1.4) eV.

For DBr photolysis, the contribution of the Br* channel is expected to be minor. Magnotta, Nesbitt, and Leone[39] reported a Br* yield of $\sim 15\%$ in the 193 nm photolysis of HBr, and Xu, Koplitz, and Wittig obtained a value of 14%.[40] Taatjes and Leone[41] measured a Br* yield of $16\% \pm 4\%$ at 212.8 nm. The faster D atoms have a higher collision frequency, which diminishes the contribution of the slower D atoms associated with the Br* photolysis channel because we measured relative rate constants, not cross sections (Sec. II A). Therefore, for a Br* yield of 15%, the measured rate constants correspond to 85% of the $E_{rel} = 1.04$ eV rate constant plus 15% of the $E_{rel} = 0.82$ eV rate constant, or 86.5% of the 1.04 eV cross section plus 13.5% of the 0.82 eV cross section.

For DI photolysis, the existence of two photolysis channels is more significant. A substantial fraction of the I atoms are produced in the electronically excited state, and the I*/I ratio varies with photolysis wavelength (i.e., with j'). Between $j' = 0$ and $j' = 15$, I*/I increases from 0.36 to 0.97.[42] Therefore, the contribution of the slow D-atom channel to the measured rate constant was 24% for $j' = 0$ and 44% for $j' = 15$. Any comparison of theoretical calculations with the measured distributions must recognize the varying contributions of these two channels.

2. D^+ production

Ions with $m/e = 2$ (D^+ or H_2^+) were observed in the TOF/MS. By flowing pure DX, H_2, and He, we found DX in combination with the high-intensity, uv REMPI laser to be the source of these unwanted (D^+) ions. (Similarly, H^+ has been observed in previous studies using HI.[20,30]) For DBr photolysis, the magnitude of the D^+ signal had a pronounced wavelength dependence in the REMPI region of interest ($\lambda = 208$–218 nm). As mentioned by KZ, D^+ ions distorted the arrival time of the HD^+ signal for some j' and therefore the data collection electronics were gated around the HD^+ peak at each j'. Interference from D^+ represented the largest source of noise in experiments using DBr for wavelengths for which the D^+ signal was relatively large ($j' \geqslant 8$). This noise arose from the overlap of the tail of the D^+ TOF peak with the HD^+ signal peak, which offset the baseline of the HD spectral peaks. In addition, this D^+ signal caused some of the spectral peaks to have a secondary maximum or "tail" beside the peak. These features were not included in the integration of the peaks, from which relative populations were obtained (representative spectral peaks are shown in Sec. II F). Noise from D^+ precluded the measurement of populations for $HD(v' = 1, j' = 1$ and $11)$. Such problems were absent when DI was used as the photolytic source of D atoms, which provided a higher S/N ratio for these experiments.

Several experimental checks were performed to investigate the possibility that systematic errors were introduced by the wavelength dependence of D^+ production in DBr photolysis. In particular, we were concerned that D^+ production could affect the measured populations by causing (1) space-charge effects; (2) depletion of the D-atom concentration; and/or (3) saturation of the multichannel plate detector. The respective experimental checks and their results were as follows:

(1) The $HD(v' = 1, j')$ rotational distribution with SRP was measured using twice the usual DBr concentration ($DI:H_2:He = 2:3:20$), i.e., doubling the D^+ concentration. This distribution agreed within experimental uncertainty with that obtained using the usual DBr concentration.

(2) The photolysis of DBr requires a single ~ 210 nm photon, whereas D^+ production requires at least three photons.[35,43] Thus, the D^+/D ratio should have a strong dependence on the pulse energy of the REMPI laser. The REMPI-laser power dependence of the $HD(v' = 1, j')$ signal from the $D + H_2$ reaction was measured for $j' = 4$ without SRP (relatively little D^+ production) and $j' = 10$ with SRP (relatively large D^+ signal). The power was varied by a factor of 3 by turning down the amplifier of the Nd:YAG laser. The results of this study are displayed in Fig. 6, in which each point represents the average of two scans over the spectral peak and the data for $j' = 4$ and $j' = 10$ have an arbitrary offset. Linear least-squares fits to a log–log plot of the data (Fig. 6) show that for $j' = 4$ ($j' = 10$), the REMPI signal is proportional to the laser pulse energy raised to the power 1.33 ± 0.06 (1.43 ± 0.10). The value of the exponent does not affect the determination of HD ($v' = 1, j'$) distribution because the power level is essentially constant over this range of product states. This test shows that the D-atom concentration was not significantly depleted as the photolysis/probe laser was tuned, although there was substantial D^+ production.

(3) The magnitude of the D^+ signal reaching the detector could be varied by changing the temporal width of the voltage pulse on the pulsed steering plate in the TOF/MS (Fig. 2). The REMPI spectral peak $HD(v' = 1, j' = 5)$ from the $D + H_2$ reaction without SRP was recorded as a function of the pulse width between 280 and 600 ns (corresponding D^+ signals of 60 to 1100 mV). No systematic

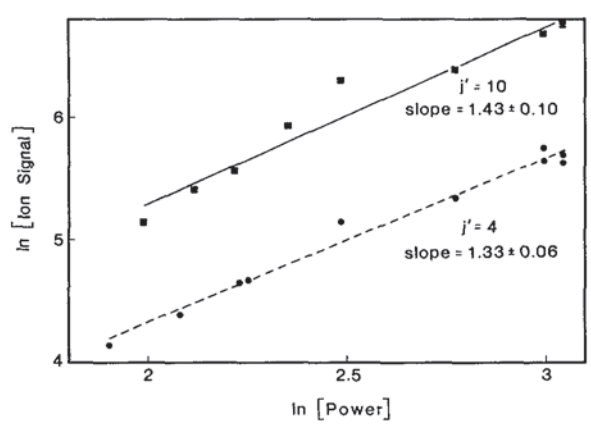

FIG. 6. Log–log plot of the REMPI signal intensity vs probe-laser pulse energy for the reaction $D + H_2 \rightarrow HD(v' = 1, j') + H$ at $E_{rel} = 1.0$ eV. The data for $j' = 4$ (without SRP) have been arbitrarily offset from those for $j' = 10$ (with SRP). Each point represents the average of two scans over the spectral peak. The lines indicate linear least-squares fits to the points.

change was observed in the integrated REMPI signal, a result indicating that the performance of the detector was not degraded by the presence of the D^+ signal.

3. Interference from the D+HX and H+DX reactions

$HD(v'=1,j')$ signal was observed when "pure DX" was flowed from the pulsed nozzle. This signal was the HD product of the reactions H + DX and D + HX, caused by the small HX impurity in the DX. The HD signal from the $D+H_2$ reaction is linear in ["DX"], whereas that from D + HX and H + DX depends quadratically on ["DX"], where "DX" denotes DX containing HX impurity. Therefore, to suppress these interfering reactions, the "DX" was made very dilute (4%–5%) in the reagent mix used for the $D+H_2$ studies. For DBr photolysis, the "DBr" was sufficiently dilute that the contribution of the D + HBr and H + DBr reactions to the total $HD(v'=1,j')$ signal was at most 5% of the smallest peak.

For DI photolysis, the $HD(v'=1,j')$ signal from the interfering reactions was less than 5% for $j'<11$ but could not be neglected for $j'>11$. It was more difficult to suppress the $HD(v'=1,$ high $j')$ signal from D(H) + HI(DI) than from D(H) + HBr(DBr) because the former reactions produce a vibrational population inversion between $v'=0$ and $v'=1$ and highly rotationally excited product,[34;44] whereas the latter ones do not.[44] For $HD(v'=1,\ j'=12,13,15)$, spectral peaks were recorded with and without Raman pumping, allowing the D(H) + HI(DI) contributions to be subtracted directly. This subtraction procedure was valid because these levels had negligible contributions from the $D+H_2(v=0)$ reaction. The subtracted contribution of the interfering reactions to the total signal was 5%, 13%, and 16% for $j'=12$, 13, and 15, respectively ($j'=14$ was not recorded because of a near coincidence; see Sec. II F). For $HD(v'=1,j'=11)$, we estimate that the D(H) + HI(DI) contribution to the total signal was less than 10% for the unpumped distribution and less than 1% for the pumped distribution. No attempt was made to subtract these minor contributions.

E. Variation of SRP efficiency

The $D+H_2(v=1,j=1)$ results using DBr photolysis were checked by varying the SRP efficiency (Sec. II C). Most of the $HD(v'=1,j')$ rotational distributions were recorded with the SRP transition nearly saturated, i.e., 50% efficiency (see Sec. II F). Some distributions were recorded with the SRP efficiency lowered to 32% by diminishing the power of the SRP Nd:YAG laser. The resultant $D+H_2(v=1,j=1)\rightarrow HD(v'=1,j')+H$ product rotational distribution was identical within experimental uncertainty to that obtained with the higher SRP efficiency.

F. Experimental procedure

$HD(v'=1,j')$ product rotational distributions for the $D+H_2$ reaction were recorded both without SRP ("unpumped" distribution) and with SRP ("pumped" distribution). For DBr photolysis, the levels $j'=0$, 2–10, 12 were scanned; for DI photolysis, the levels $j'=0$–13, 15 were

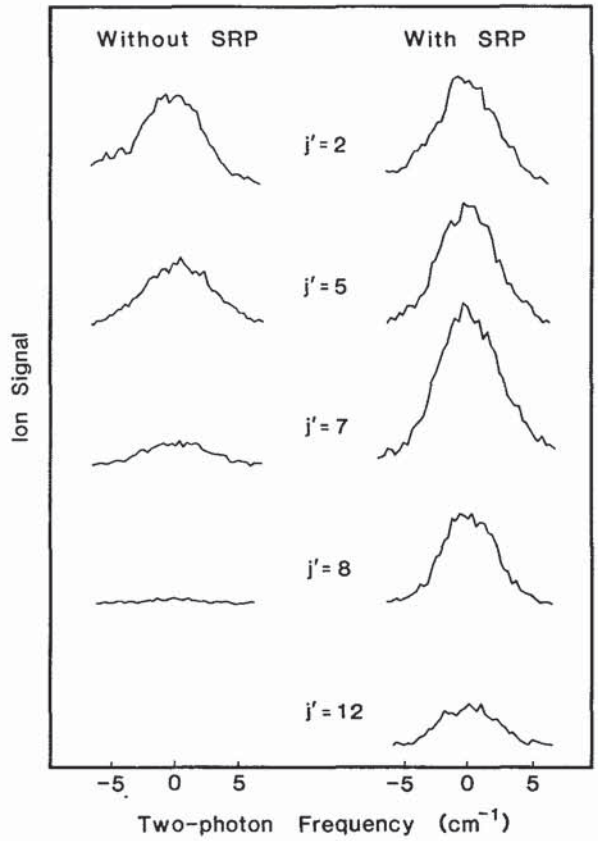

FIG. 7. Representative spectral peaks for the $HD(v'=1,j')$ product of the $D+H_2$ reaction without SRP (left column) and with SRP (right column). The D atoms were generated by photolysis of DBr. Each peak represents one scan, which took 90–120 s; see the text for additional experimental conditions. All peaks were recorded on the same day. On the abscissa, 0 denotes line center.

scanned. Spectral peaks were recorded with a time constant of 1.5–2.0 s (1.5–2.0 min per peak). Representative spectral peaks for the unpumped and pumped distributions using DBr photolysis are shown in Fig. 7, and those for DI photolysis are shown in Fig. 8. All of the peaks displayed in each figure were recorded on a single day, so their areas reflect the relative populations of the $HD(v'=1,j')$ rotational levels. An example of a tail caused by D^+ production in the photolysis of DBr (Sec. II D 2) is shown in Fig. 7 on the left-hand side of the $j'=2$ peak.

The pumped and unpumped distributions were each recorded 15–20 times on 4–6 separate days. On a given day, 3–5 pumped and unpumped distributions were recorded. The SRP efficiency (Sec. II C) was determined both before and after recording the pumped distributions by measuring with REMPI the SRP depletion of $H_2(v=0,j=1)$ (see Fig. 4). The SRP efficiency was at least 45% for all of the data reported here. Specifically, the SRP efficiency was $47.7\% \pm 2.0\%$ for the experiments using DBr photolysis and $47.4\% \pm 2.2\%$ for those using DI photolysis. The corresponding fractions of the total population excited into $v=1$ are 33.9% (33.7%) for DBr (DI) photolysis.

The pumped distributions contain contributions from both $H_2(v=0)$ and $H_2(v=1)$ reagents. To extract the $D+H_2(v=1,j=1)\rightarrow(v'=1,j')+H$ state-to-state prod-

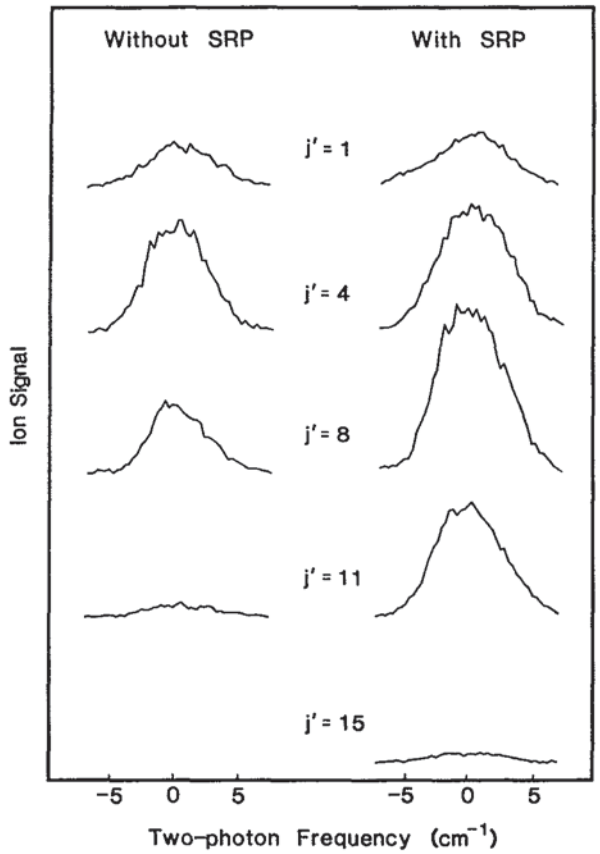

FIG. 8. Same as Fig. 7, but for DI photolysis.

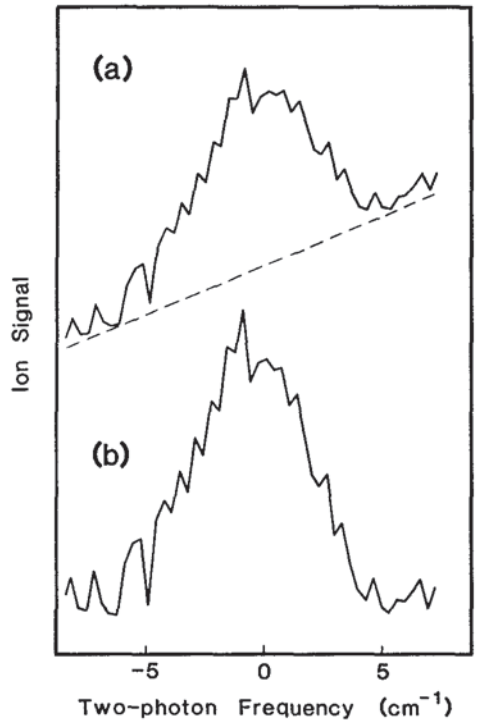

FIG. 9. (a) Representative spectral peak of the $HD(v'=1,j'=6)$ product of the $D+H_2$ reaction (with SRP) at $E_{rel}=1.0$ eV. The sloped baseline was caused by the proximity of the $H_2(v=1,j=1)$ spectral peak. (b) Same as (a), but with the sloped baseline subtracted. Such baseline-corrected peaks were used in determining relative populations for the $HD(v'=1, j'=6)$ product of the pumped reactions. On the abscissa, 0 denotes line center.

uct rotational distribution from the measured distributions, we had to remove the $H_2(v=0)$ contribution to the pumped distribution (see Sec. III A below). This subtraction procedure required a knowledge of the relative magnitudes of the pumped and unpumped distributions, i.e., the pumped and unpumped distributions had to be "locked" together. This locking was performed by measuring the SRP enhancement of a given $HD(v'=1)$ rotational level. The levels used were $j'=7$ for DBr photolysis and $j'=8$ for DI photolysis. The SRP enhancement of these levels was measured each day that pumped distributions were recorded, both before and after recording the pumped distributions. The measured enhancements were 6.12 ± 0.45 for $j'=7$ (DBr photolysis) and 2.28 ± 0.11 for $j'=8$ (DI photolysis).

The dichroic mirrors (Virgo Optical) used to direct the photolysis/probe beam into the vacuum chamber (Fig. 1) cover a spectral region that includes $H_2(v=0,j=1)$ (for measuring the SRP efficiency) and $HD(v'=1,j'=0\text{–}12)$. Thus this one set of mirrors was sufficient for all of the measurements using DBr photolysis. For DI photolysis, the pumped distribution was measured up to $j'=15$, for which a second set of dichroic mirrors was required. $HD(v'=1, j'=0\text{–}12)$ spectral peaks were recorded using the first set of mirrors, and $HD(v'=1, j'=12\text{–}15)$ spectral peaks were subsequently recorded using the second set. Since the low j' and high j' distributions were overlapped at $j'=12$, they could be combined into a single distribution.

The $HD(v'=1,j'=14)$ spectral peak could not be recorded because it overlaps with the $HD(v'=2,j'=1)$ spectral peak in the $(2+1)$ REMPI detection scheme. This overlap has prevented us from measuring $HD(v'=2, j'=1)$ populations in previous experiments.[28] Similarly, $HD(v=1,j=6)$ and $H_2(v=1,j=1)$ are in close spectroscopic proximity (within 2 Å). A high density of $H_2(v=1, j=1)$ was prepared in the reaction volume by SRP, causing H_2^+ ions from REMPI of this level to spill over into $m/e=3$ (HD^+) in the TOF. Because of this overlap, $HD(v'=1,j'=6)$ spectral peaks from the pumped reaction had a sloped baseline, i.e., the $HD(v'=1,j'=6)$ peaks were superimposed on the tail of the $H_2(v=1,j=1)$ peak [Fig. 9(a)]. The sloped baseline was subtracted from the $HD(v'=1,j'=6)$ peaks [Fig. 9(b)] before they were integrated. Interference from H_2^+ could result in loss of $HD(v'=1,j'=6)$ REMPI signal via the mechanisms discussed in Sec. II D 2 in connection with D^+. The measured $HD(v'=1,j'=6)$ populations for the pumped $D+H_2$ reactions therefore represent lower bounds on the actual populations.

III. RESULTS AND DISCUSSION

A. Distributions

Figure 10(a) shows the $HD(v'=1,j')$ rotational distributions for the $D+H_2$ reaction at $E_{rel}=1.0$ eV measured without SRP (unpumped reaction, dashed curve) and with SRP (pumped reaction, solid curve). The contribution of the $D+H_2(v=0)$ reaction to the pumped distribution

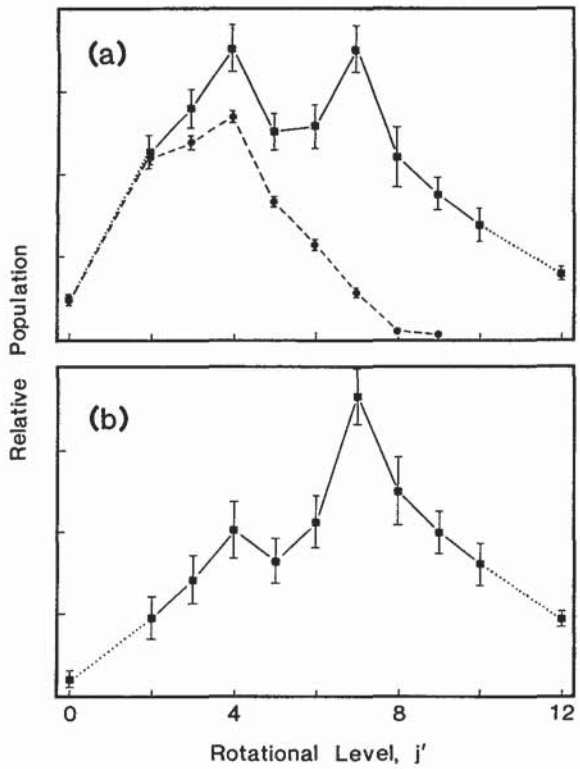

FIG. 10. Rotational population distributions of the $HD(v'=1,j')$ product from the reaction $D+H_2$ at $E_{rel}=1.0$ eV. Error bars represent one standard deviation; where not shown, the error bar is the size of the point. (a) The circles connected by dashed lines show the unpumped distribution from the reaction $D+H_2(v=0,j)$ and the squares connected by solid lines show the pumped distribution measured after SRP of the H_2 reagent. (b) The distribution from the reaction $D+H_2(v=1,j=1)$ obtained by subtracting 66% of the unpumped distribution from the pumped distribution (see Sec. III A). Dotted lines connect the populations of levels adjacent to a level for which the population was not measured (see the text).

must be subtracted to obtain the product rotational distribution for the $D+H_2(v=1,j=1)$ reaction. Figure 10(b) shows the $D+H_2(v=1,\ j=1)\rightarrow HD(v'=1,\ j')+H$ state-to-state distribution obtained by subtracting 66.1% of the unpumped distribution from the pumped distribution; the 66.1% takes into account the 33.9% depletion of $H_2(v=0)$ by SRP. The error bars denote one standard deviation and, in Fig. 10(b), include uncertainties in the measured distributions [Fig. 10(a)], in the measurement of the SRP efficiency (Secs. II C and II F), and in the locking of the pumped and unpumped distributions (Sec. II F). The results displayed in Fig. 10 are listed in Table I. Corresponding results for the $D+H_2$ reaction at $E_{rel}=1.4$ eV are presented in Fig. 11 and Table II.

The subtraction procedure by which the $D+H_2(v=1,\ j=1)\rightarrow HD(v'=1,\ j')+H$ product rotational distributions [Figs. 10(b) and 11(b)] were extracted from the measured distributions [Figs. 10(a) and 11(a)] contains the assumption that integral cross sections for the reaction $D+H_2(v=0,\ j)\rightarrow HD(v'=1,\ j')+H$ have no dependence on j. This assumption is required because SRP perturbs the $H_2(v=0,j)$ rotational distribution by pumping population out of a single rotational level ($j=1$). We have tested this assumption by measuring the $HD(v'=1,\ j')$ product rotational distribution from the $D+$*para*-$H_2(v=0,j)$ reaction. Both SRP and the use of *para*-H_2 (p-H_2) deplete $H_2(v=0,\ j=1)$. Thus substituting p-H_2 for *normal*-H_2 (n-H_2) provides a perturbation on the $H_2(v=0,\ j)$ reagent rotational distribution that is similar to, but more pronounced than, that caused by SRP. The p-H_2 used in these measurements had a purity of $\sim 85\%$ as measured by REMPI. This purity is somewhat lower than that of previous experiments[23] on the $H+p$-H_2 reaction because p-H_2 degraded more quickly in the pulsed nozzle than in the capillary nozzle. A purity of 85% is sufficient to test the subtraction procedure. The $HD(v'=1,j')$ distributions obtained using n-H_2 and p-H_2 are compared in Fig. 12. They are identical within the relatively small experimental uncertainty. This result was not unexpected[6,45] but provides direct experimental verification that the subtraction procedure did not introduce errors into the extraction of the state-to-state distributions from the measurements. This comparison appears to be the first experimental demonstration that integral cross sections for the reaction $D+H_2(v=0,\ j)\rightarrow HD(v'=1,\ j')+H$ have at most a weak dependence on j for the rotational levels populated at moderate temperatures.

TABLE I. Product rotational distributions for the reaction $D+H_2(v,j)\rightarrow HD(v'=1,j')+H$ at $E_{rel}=1.04$ and 0.82 eV.

j'	Unpumped ($v=0,j$)	Pumped ($v=0$ and 1)	($v=1,j=1$)	Previous[a] ($v=0,j$)
0	0.41 ± 0.06	0.20 ± 0.03	0.11 ± 0.06	0.46 ± 0.02
1	...	...	...	1.21 ± 0.05
2	1.94 ± 0.07	0.95 ± 0.06	0.50 ± 0.14	1.71 ± 0.07
3	2.11 ± 0.08	1.17 ± 0.06	0.74 ± 0.16	1.99 ± 0.09
4	2.39 ± 0.07	1.48 ± 0.06	1.06 ± 0.19	2.14 ± 0.08
5	1.47 ± 0.05	1.05 ± 0.06	0.86 ± 0.14	1.55 ± 0.07
6	1.01 ± 0.06	1.08 ± 0.08	1.11 ± 0.17	1.07 ± 0.08
7	0.51 ± 0.05	1.47 ± 0.06	1.91 ± 0.18	0.71 ± 0.06
8	0.10 ± 0.03	0.93 ± 0.14	1.31 ± 0.22	0.25 ± 0.02
9	0.05 ± 0.03	0.74 ± 0.07	1.05 ± 0.13	0.120 ± 0.017
10	...	0.58 ± 0.08	0.85 ± 0.13	...
11	...	...	...	...
12	...	0.34 ± 0.03	0.50 ± 0.05	...

[a] Reference 22.

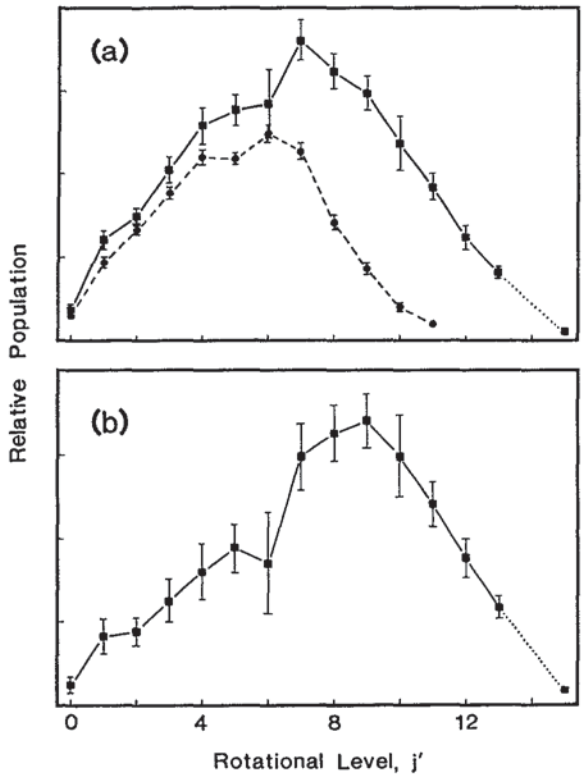

FIG. 11. Same as Fig. 10, but at $E_{rel} = 1.4$ eV. The kink and relatively large error bar at $j' = 6$ for the pumped distribution in (a) and for (b) are probably caused by interference from $H_2(v=1, j=1)$; see Sec. II F.

The distribution shown in Fig. 10(b) from the reaction $D + H_2(v=1, j=1)$ at $E_{rel} = 1.0$ eV may be bimodal with a secondary peak at $j' = 4$. This kink, however, is barely at the level of statistical significance. Recall that in the 210 nm photolysis of DBr, ~15% of the D atoms are produced in coincidence with Br* ($E_{rel} = 0.82$ eV, see Sec. II D *1*). This group of slower D atoms may be responsible for the kink at $j' = 4$. This interpretation is tentative because the secondary peak is within experimental uncertainty and because theoretical calculations are not available at both the collision energies necessary to test it.

B. Energy disposal

From the distributions presented in Tables I and II, first moments ($\langle j' \rangle$) and fractions of the available energy appearing as product rotation (f_R and g_R)[31] can be calculated according to

$$\langle j' \rangle = \sum_{j'} j' P(j'), \tag{2}$$

$$f_R = \sum_{j'} P(j') E(j')/E, \tag{3}$$

and

$$g_R = \sum_{j'} P(j') E(j')/[E - E(v')], \tag{4}$$

where $P(j')$ is the relative population of the $HD(v',j')$ product level for the reaction $D + H_2(v, j) \rightarrow HD(v', j') + H$; $E(j')$ and $E(v')$ are the rotational and vibrational energy, respectively, of that level;[35] and E is the total available energy. The normalization assumed in Eqs. (2)–(4) is

$$\sum_{j'} P(j') = 1. \tag{5}$$

The values of E, $\langle j' \rangle$, f_R, and g_R for reactions $D + H_2(v=0, j)$ and $D + H_2(v=1, j=1)$ at $E_{rel} = 1.0$ and 1.4 eV are given in Tables III and IV, respectively.

The available energy E is the sum of the collision energy, the reagent internal energy, and the reaction exothermicity.[35] The higher collision energy associated with production of ground state X atoms in DX photolysis was used in calculating E. For the $D + H_2(v=0, j)$ reactions, the reagent internal energy was 103 cm^{-1}, which is the average rotational energy of $H_2(v=0)$ at 150 K. For the $D + H_2(v=1, j=1)$ reactions, the reagent internal energy was 4274 cm^{-1}. Because populations of all energetically accessible levels were not measured in the present experi-

TABLE II. Product rotational distributions for the reaction $D + H_2(v,j) \rightarrow HD(v'=1,j') + H$ at $E_{rel} = 1.38$ and 0.92 eV.

j'	Unpumped ($v=0, j$)	Pumped ($v=0$ and 1)	($v=1, j=1$)
0	0.182 ± 0.017	0.12 ± 0.02	0.09 ± 0.04
1	0.57 ± 0.04	0.41 ± 0.04	0.31 ± 0.07
2	0.80 ± 0.04	0.50 ± 0.03	0.33 ± 0.06
3	1.07 ± 0.05	0.69 ± 0.05	0.47 ± 0.10
4	1.34 ± 0.06	0.87 ± 0.06	0.60 ± 0.13
5	1.33 ± 0.05	0.94 ± 0.05	0.71 ± 0.11
6	1.52 ± 0.07	0.96 ± 0.14	0.64 ± 0.23
7	1.39 ± 0.06	1.22 ± 0.06	1.12 ± 0.15
8	0.87 ± 0.06	1.10 ± 0.05	1.22 ± 0.13
9	0.53 ± 0.05	1.01 ± 0.06	1.27 ± 0.12
10	0.26 ± 0.03	0.80 ± 0.11	1.12 ± 0.18
11	0.133 ± 0.013	0.63 ± 0.05	0.91 ± 0.10
12	···	0.43 ± 0.05	0.67 ± 0.09
13	···	0.28 ± 0.03	0.45 ± 0.05
14	···	···	···
15	···	0.049 ± 0.005	0.077 ± 0.009

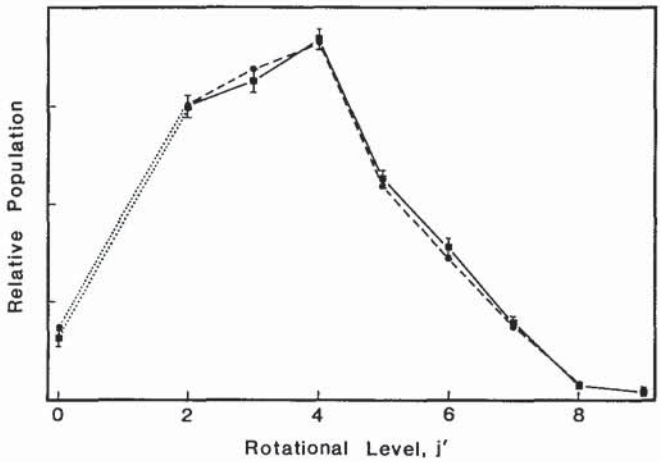

FIG. 12. Rotational population distributions of the $HD(v'=1,j')$ product from the reaction $D+H_2(v=0,j)$ at $E_{rel}=1.0$ eV. The squares connected by solid lines are for n-H_2 (i.e., 25% p-H_2) reagent and the circles connected by dashed lines are for 85% purity p-H_2 reagent. Dotted lines connect the populations of levels adjacent to a level for which the population was not measured (see the text). Error bars representing one standard deviation are shown for the $D+n$-H_2 distribution; uncertainties associated with the $D+p$-H_2 distribution are comparable.

ment, the following approximations were used in calculating $\langle j'\rangle$, f_R, and g_R: (1) for levels missing from within the distributions ($j'=1$ and 11 for DBr photolysis, $j'=14$ for DI photolysis), populations were obtained by linearly interpolating the populations of the two adjacent levels, and (2) for levels beyond the ranges of the measured distributions, the populations were taken as zero. These approximations are not expected to affect substantially the calculated energy-disposal parameters.

From a knowledge of the relative magnitudes of the pumped and unpumped distributions, we can calculate the enhancement in the $HD(v'=1)$ reaction rate (specific cross section) that occurs upon reagent vibrational excitation according to

$$\sigma_{11}/\sigma_{01}=\frac{\Sigma_{j'}P(v=1;v'=1,j')}{\Sigma_{j'}P(v=0;v'=1,j')}, \tag{6}$$

where $\sigma_{vv'}$ denotes the rate of the reaction $D+H_2(v,j)\rightarrow HD(v'=1,\text{all}\,j')+H$ and $P(v;v',j')$ is the relative population of the $HD(v',j')$ product level when the H_2 reagent is initially in the vibrational state v. The two approximations discussed in the previous paragraph were used in calculating σ_{11}/σ_{01}. Values of the vibrational enhancement at $E_{rel}=1.0$ and 1.4 eV are given in Tables III and IV, respectively.

The distributions presented in Figs. 9 and 10 and the energy-disposal parameters listed in Tables III and IV show that vibrational excitation of the H_2 reagent results in substantial rotational excitation of the $HD(v'=1)$ product of the $D+H_2$ reaction. This substantial excitation is not simply an energetic effect, as is clear from the g_R values. For the $D+H_2$ reaction at $E_{rel}=1.0$ eV, excitation of the H_2 reagent from $v=0$ to $v=1$ increases g_R by 71%, and at $E_{rel}=1.4$ eV the increase is 38%. This diminished effect of vibrational excitation upon increased translational energy is expected because the fraction of E that is provided by reagent vibrational energy is decreased when E_{rel} is increased. A similar effect is seen in the σ_{11}/σ_{01} values.

Preferential disposal of the available energy into product rotation upon regent vibrational excitation is demonstrated by comparing g_R values for the reactions $D+H_2(v=0,\ j)$ at $E_{rel}=1.4$ eV ($E=1.4$ eV) and $D+H_2(v=1,j=1)$ at $E_{rel}=1.0$ eV ($E=1.6$ eV). The available energy E is nearly equal for these two reactions, but the contributions of reagent translation and vibration to E are very different. For the reaction $D+H_2(v=0,j)$ g_R is 0.197 ± 0.006, whereas for the reaction $D+H_2(v=1,j=1)$ g_R is 0.263 ± 0.019. Thus transfer of 0.5 eV from reagent translation to H_2 vibration increases g_R by $34\pm10\%$.

TABLE III. Energy-disposal parameters for the reaction $D+H_2(v,j)\rightarrow HD(v'=1,j')+H$ at $E_{rel}=1.04$ and 0.82 eV.

	Experiment		QM calculations		QCT calculations	
	$(v=0,j)$	$(v=1,j=1)$	$(v=0,j)$[a]	$(v=1,j=1)$[b]	$(v=0,j)$[c]	$(v=1,j=1)$[b]
$E(\text{cm}^{-1})$[d]	8860	12 950	8850 (8750)	12 790	8870	12 870
$\langle j'\rangle$[e]	3.51 ± 0.07	6.7 ± 0.3	3.57 (3.81)	8.10	4.42 ± 0.10	8.25 ± 0.10
f_R[f]	0.091 ± 0.003	0.189 ± 0.013	0.094 (0.107)	0.258	0.133 ± 0.004	0.265 ± 0.005
g_R[g]	0.154 ± 0.005	0.263 ± 0.018	0.159 (0.183)	0.360	0.225 ± 0.007	0.370 ± 0.007
σ_{11}/σ_{01}[h]	4.2 ± 0.3		7.03		4.43 ± 0.08	

[a] Reference 6 (entries in parentheses are from Ref. 8).
[b] Reference 5.
[c] Reference 47.
[d] The differences in the theoretical values are because of slightly different initial conditions.
[e] Equation (2).
[f] Equation (3).
[g] Equation (4).
[h] Equation (6).

TABLE IV. Energy-disposal parameters for the reaction $D + H_2(v, j) \rightarrow HD(v' = 1, j') + H$ at $E_{rel} = 1.38$ and 0.92 eV.

	$(v=0,j)$	$(v=1,j=1)$
$E(cm^{-1})$	11 680	15 690
$\langle j' \rangle$[a]	5.20 ± 0.10	7.9 ± 0.4
f_R[b]	0.136 ± 0.004	0.208 ± 0.013
g_R[c]	0.197 ± 0.006	0.271 ± 0.017
σ_{11}/σ_{01}[d]	3.4 ± 0.2	

[a] Equation (2). [c] Equation (4).
[b] Equation (3). [d] Equation (6).

KZ and BZTSK have discussed mechanisms contributing to the enhanced rotational excitation of the $HD(v' = 1)$ product of the $D + H_2$ reaction that occurs upon reagent vibrational excitation. The H_3 bend potential, which has a minimum for collinear geometry, is sensitive to the H_2 reagent bond length and becomes shallower upon elongation of the H–H bond.[46] This opening of the reactive cone of acceptance allows reaction to occur for highly bent trajectories and for collisions with large impact parameters, both of which can produce rotationally excited product molecules.[31] BZTSK found that the opacity function for the reaction $D + H_2(v,j) \rightarrow HD(v' = 1, \text{all } j') + H$ was extremely sensitive to reagent vibrational excitation. For $H_2(v = 0, j = 1)$, the reaction probability peaked at an impact parameter of $b = 0$ (head-on collision), monotonically decreased with increasing b, and was nearly zero by $b = 1$ Å. For $H_2(v = 1, j = 1)$, the reaction probability peaked at $b \approx 0.8$ Å (orbital angular momentum $l = 17\hbar$), and $b = 1$ Å ($l = 22\hbar$) collisions had comparable reactivity to $b = 0$ collisions. BZTSK concluded that the larger amount of "angular momentum available to the products in high-l reactions provides a reasonable explanation of the higher $\langle j' \rangle$ observed...when H_2 is initially vibrationally excited."[5]

Although the collision energies are different for the experiments using DBr and DI photolysis, they are sufficiently similar that the results can be compared. The values collected in Tables III and IV demonstrate that the two D-atom sources yielded very similar results for energy disposal in the reactions $D + H_2(v = 0, j)$ and $D + H_2(v = 1, j = 1)$ and for the effect of vibrational excitation upon the dynamics. An interesting observation is provided by (perhaps artificially) separating the different contributions to the available energy E. Assume that a constant fraction of E that is not reagent vibration appears as product rotational energy at each E_{rel} (9.1% at $E_{rel} = 1.0$ eV and 13.6% at $E_{rel} = 1.4$ eV, obtained from the unpumped reactions), and subtract this energy from the rotational energy of the $HD(v' = 1)$ product of the $D + H_2(v = 1, j = 1)$ reaction. Then, the remaining product rotational energy must originate as reagent vibrational energy. This remaining energy is the same at both collision energies (~ 1700 cm^{-1}) and corresponds to $41\% \pm 5\%$ of the reagent vibrational energy. While intriguing, the dynamical significance of this observation cannot be assessed from only two experiments at similar collision energies. Nonetheless, it highlights the consistency of the results obtained using DBr and DI photolysis.

C. Comparison with previous experiments

The present results at $E_{rel} = 1.0$ eV can be compared with the previous measurements of Kliner, Rinnen, and Zare[22] for $D + H_2(v = 0, j)$ and of KZ for $D + H_2(v = 1, j = 1)$. For the unpumped $D + H_2(v = 0, j)$ reaction, the present $HD(v' = 1, j')$ product rotational distribution is in close agreement with that obtained previously, as shown in Fig. 13(a) and Table I. The distributions have been normalized to the sum of the common populations. This comparison provides further evidence that the incorporation of the pulsed nozzle (Sec. II B) did not introduce errors into the experiment.

A comparison of the present $D + H_2(v = 1, j = 1) \rightarrow HD(v' = 1, j') + H$ product rotational distribution with that obtained from the preliminary measurement is shown in Fig. 13(b), again normalizing the distributions to the sum of the common populations. The agreement is generally good, with both distributions peaking at $j' = 7$. However, the present distribution is somewhat colder rotationally. We attribute this change to the improved S/N in the present experiment. In particular, the improvement of the SRP efficiency and stability (Sec. II C) permitted a more

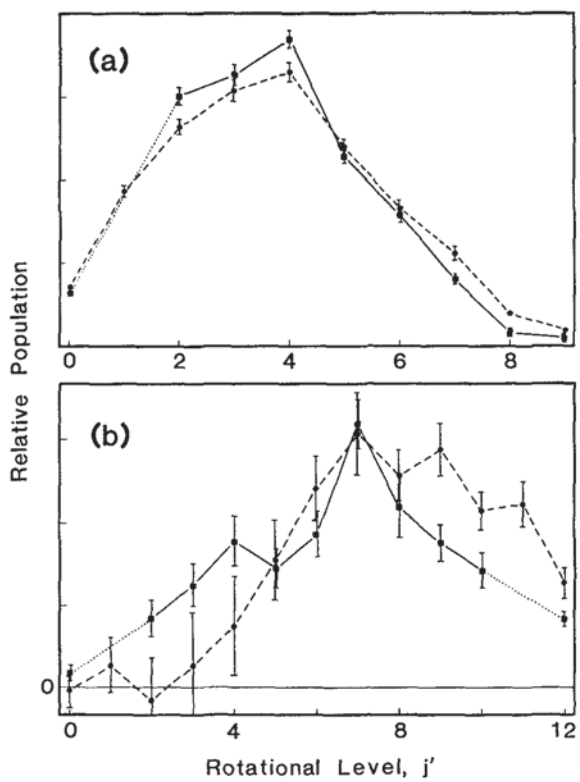

FIG. 13. Comparison of present (squares connected by solid lines) and previous (circles connected by dashed lines) rotational population distributions of the $HD(v' = 1, j')$ product from the reaction $D + H_2(v, j)$ at $E_{rel} = 1.0$ eV: (a) $H_2(v = 0, j)$ (previous distribution from Ref. 22) and (b) $H_2(v = 1, j = 1)$ (previous distribution from Ref. 21). Error bars represent one standard deviation. Note that in (b) the position of zero population is not located on the abscissa because two of the previous populations were slightly negative (with error bars including zero). Dotted lines connect the populations of levels adjacent to a level for which the population was not measured (see the text).

reliable determination of this distribution. Populations of levels with $j' < 5$ were zero within experimental uncertainty in the previous experiment. The present value of σ_{11}/σ_{01} (4.2 ± 0.3) agrees with the preliminary value of $\geqslant 4$.

Populations of the levels $HD(v'=1, j'=1$ and $11)$ were measured in the previous experiments. With the present apparatus, measurement of these levels was precluded by increased interference from D^+ ions (Sec. II D 2), perhaps because of higher DBr concentration from the pulsed nozzle.

D. Comparison with theory

The experimental $HD(v'=1,j')$ product rotational distributions for the reactions $D+H_2(v=0,j)$ and $D+H_2(v=1,j=1)$ at $E_{rel}=1.0$ eV can be compared with those derived from both QM and quasiclassical trajectory (QCT) calculations. Calculated and measured energy-disposal parameters (Sec. III B) are compared in Table III. To make the experimental and theoretical values in this table consistent, each theoretical distribution was truncated at the highest value of j' present in the corresponding experimental distribution before energy-disposal parameters were calculated. Similarly, in subsequent figures, experimental and theoretical rotational population distributions have been normalized to the sum of the common populations. Theoretical results are not available for comparison with the experiment at $E_{rel}=1.4$ eV.

1. Quasiclassical trajectory calculations

As has been reported,[22] a QCT calculation by Blais and Truhlar[47] reproduced the shape of the product rotational distribution for the reaction $D+H_2(v=0,j)$ but was too hot by about one quantum. A comparison of the $D+H_2(v=1,j=1)\rightarrow HD(v'=1,j')+H$ product rotational distributions derived from experiment and from the QCT calculation of BZTSK is shown in Fig. 14. The calculated distribution is again too hot rotationally. The measured distribution peaks at $j'=7$, whereas the QCT distribution peaks at $j'=11$. The σ_{11}/σ_{01} value obtained from the QCT calculation (4.43 ± 0.08) is in close agreement with experiment (4.2 ± 0.3).

2. Quantum-mechanical calculations

The product rotational distribution for the reaction $D+H_2(v=0,j)$ at $E_{rel}=1.0$ eV (Ref. 22) was quantitatively reproduced by two QM calculations.[6,8] As discussed in the Introduction, preliminary measurements indicated that such agreement may not persist when the reagent is vibrationally excited. A comparison of the present $D+H_2(v=1, j=1)\rightarrow HD(v'=1,j')+H$ state-to-state distribution with that obtained from the QM calculation of BZTSK is shown in Fig. 15(a). The calculated distribution qualitatively reproduces the measured shift in the product rotational distribution upon reagent vibrational excitation, but there are differences between the calculated and measured distributions that are outside of experimental uncertainty. The theoretical distribution peaks at $j'=10$, whereas the measured distribution peaks at $j'=7$.

The energy-disposal parameters given in Table III also demonstrate the similarities and differences between QM theory and experiment. A very pronounced discrepancy is found for the increase in the $HD(v'=1)$ rate constant upon reagent vibrational excitation $(\sigma_{11}/\sigma_{01})$. The experimental value is 4.2 ± 0.3, whereas the QM value is 7.03, which is 67% larger than the measurement.

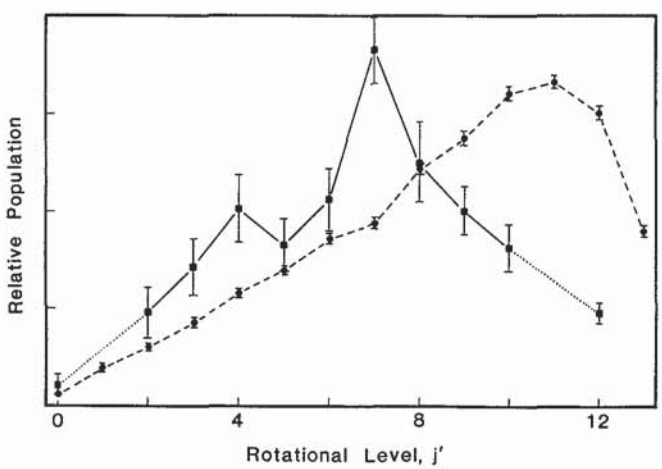

FIG. 14. Comparison of experimental (squares connected by solid lines) and quasiclassical (circles connected by dashed lines, Ref. 5) rotational population distributions for the $HD(v'=1,j')$ product from the reaction $D+H_2(v=1,j=1)$ at $E_{rel}=1.0$ eV. Error bars represent one standard deviation; where not shown, the error bar is the size of the point.

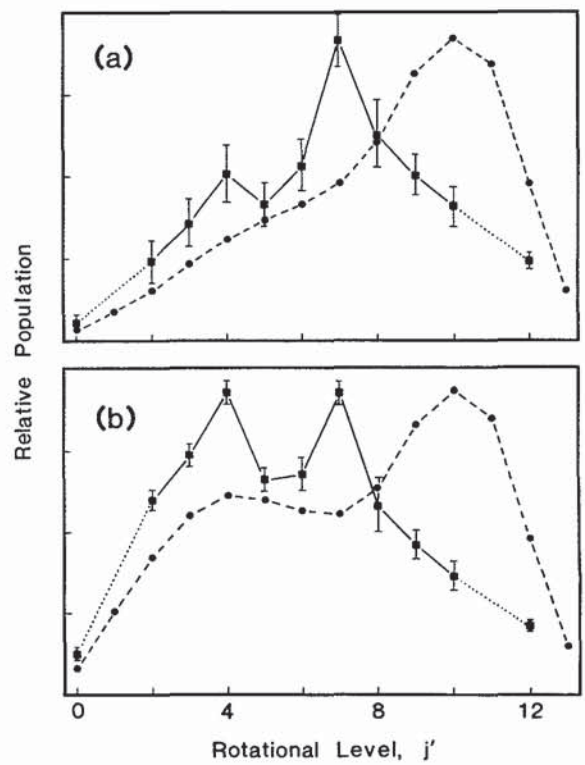

FIG. 15. Comparison of experimental (squares connected by solid lines) and quantum-mechanical (circles connected by dashed lines, Ref. 5) rotational population distributions for the $HD(v'=1,j')$ product from the reaction $D+H_2(v,j)$ at $E_{rel}=1.0$ eV. Error bars represent one standard deviation. (a) H_2 $(v=1,j=1)$ and (b) H_2 $(v=0$ and $1)$ pumped reaction; see Sec. III A. Dotted lines connect the populations of levels adjacent to a level for which the population was not measured (see the text).

The $D + H_2(v = 1, j = 1) \rightarrow HD(v' = 1, j') + H$ product rotational distribution was extracted from the measured pumped and unpumped distributions (Sec. III A). Alternatively, to compare theory with experiment, the theoretical distributions can be combined to simulate the measured distribution from the pumped $D + H_2(v = 0$ and $1)$ reaction [Fig. 10(a), solid curve]. This simulation, based on the QM calculations of BZTSK, is compared with the measured distribution in Fig. 15(b). Both the experimental and theoretical pumped distributions are bimodal with the first peak at $j' = 4$. The second peak, however, is larger in the QM calculation than in the experiment and occurs at $j' = 10$ rather than $j' = 7$.

The experimental checks and characterizations reported in Sec. II give us confidence that the measured distributions represent the unrelaxed reaction product and that these distributions have been determined accurately. The reported error bars contain contributions from all measurable sources of uncertainty (Sec. III A) and reflect many measurements of the distributions. The assumption used in extracting the state-to-state distribution from the measured distributions was tested by substituting p-H_2 for n-H_2 (Sec. III A). A verification of the $D + H_2$ results at $E_{rel} = 1.0$ eV (DBr photolysis) was provided by the experiments using DI photolysis, as discussed in Sec. III B.

Although the measured distributions using DBr photolysis ($E_{rel} = 1.04$ eV) have a contribution from the Br* channel ($E_{rel} = 0.82$ eV), this contribution is only $\sim 13.5\%$ (Sec. II D *1*). Therefore, neglect of this channel is unlikely to be the cause of the disagreement between QM theory and experiment. The primary difference between the QM calculation and the experiment is that the experiment had a spread in E_{rel} of ~ 0.15 eV FWHM. This spread was caused by thermal motions of the reagents (estimated to be ~ 0.07 eV, Sec. II B) and by the use of a tunable photolysis source (0.08 eV, Sec. II D *1*). If QM calculations over the experimentally accessed energy range were available, an accurate simulation of the experiment could be performed by convolving the theoretical cross sections with the experimental energy width, as was done for $H + p$-H_2.[23] Nonetheless, the discrepancy shown in Fig. 15 is unlikely to be solely attributed to the experimental energy spread, as evidenced by previous comparisons of experiment with QM and QCT calculations performed at fixed values of E_{rel}.[5,8,11,20,22,48] We conclude that a real disagreement exists between the best available QM calculations and the present experimental measurements of integral cross sections for the reaction $D + H_2(v = 1, j = 1)$ at $E_{rel} = 1.0$ eV.

Despite our best efforts to find fault with the experiment, some unknown experimental artifact may exist and be responsible for the discord between theory and experiment. This possibility suggests that we and others should perform additional experiments involving vibrationally excited reagents. The measurements using DI reported here provide the first such experiments. Alternatively, theory may need to be improved. The necessary improvements could be trivial, such as the detection of an error in the computer code. Although many QM calculations for the $H + H_2$ reaction family have been verified independently by several groups,[9] the computations of BZTSK, which are the highest-energy QM calculations to date, have not been. Possibly, the necessary improvements are nontrivial. For example, the H_3 PES may need to be refined. The present experiment can access nuclear configurations that are far removed from the minimum energy path and for which there are relatively few *ab initio* points. Such a reevaluation of the bend potential was recently reported by Bauschlicher, Langhoff, and Partridge.[49] Another possibility, which has been suggested by Lepetit and Kuppermann,[50] is that nonadiabatic effects arising from the conical intersection between the H_3 ground and first electronically excited states must be included. Further comparisons between theory and experiment are required before it can be said that the simplest chemical reaction is fully understood.

ACKNOWLEDGMENTS

We are grateful to C. A. Taatjes and S. R. Leone for measuring the Br*/Br ratio in the 212.8 nm photolysis of DBr (Ref. 41) and to I. Levy and M. Shapiro for providing a tabulation of their calculated I*/I ratios in the photolysis of DI (Ref. 42). This work was supported by the National Science Foundation under NSF CHE-89-21198.

[1] M. R. Cohen and E. Nagel, *An Introduction to Logic and Scientific Method* (Harcourt, Brace, New York, 1934).
[2] J. T. Davies, *The Scientific Approach* (Academic, New York, 1965).
[3] C. W. Bauschlicher, Jr. and S. R. Langhoff, Chem. Rev. (in press).
[4] M. Mladenovic, M. Zhao, D. G. Truhlar, D. W. Schwenke, Y. Sun, and D. J. Kouri, J. Phys. Chem. **92**, 7035 (1988).
[5] N. C. Blais, M. Zhao, D. G. Truhlar, D. W. Schwenke, and D. J. Kouri, Chem. Phys. Lett. **166**, 11 (1990).
[6] M. Zhao, D. G. Truhlar, D. W. Schwenke, and D. J. Kouri, J. Phys. Chem. **94**, 7074 (1990).
[7] J. Z. H. Zhang and W. H. Miller, Chem. Phys. Lett. **153**, 465 (1988).
[8] J. Z. H. Zhang and W. H. Miller, J. Chem. Phys. **91**, 1528 (1989).
[9] W. H. Miller, Annu. Rev. Phys. Chem. **41**, 245 (1990), and references therein.
[10] D. E. Manolopoulos and R. E. Wyatt, Chem. Phys. Lett. **159**, 123 (1989).
[11] M. D'Mello, D. E. Manolopoulos, and R. E. Wyatt, J. Chem. Phys. (submitted).
[12] J. M. Launay and M. Le Dourneuf, Chem. Phys. Lett. **163**, 178 (1989).
[13] D. P. Gerrity and J. J. Valentini, J. Chem. Phys. **81**, 1298 (1984).
[14] H. B. Levene, D. L. Phillips, J.-C. Nieh, D. P. Gerrity, and J. J. Valentini, Chem. Phys. Lett. **143**, 317 (1988).
[15] G. W. Johnston, B. Katz, K. Tsukiyama, and R. Bersohn, J. Phys. Chem. **91**, 5445 (1987).
[16] R. Götting, V. Herrero, J. P. Toennies, and M. Vodegel, Chem. Phys. Lett. **137**, 524 (1987).
[17] S. A. Buntin, C. F. Giese, and W. R. Gentry, J. Chem. Phys. **87**, 1443 (1987).
[18] S. A. Buntin, C. F. Giese, and W. R. Gentry, Chem. Phys. Lett. **168**, 513 (1990).
[19] R. E. Continetti, B. A. Balko, and Y. T. Lee, J. Chem. Phys. **93**, 5719 (1990).
[20] K.-D. Rinnen, D. A. V. Kliner, and R. N. Zare, J. Chem. Phys. **91**, 7514 (1989).
[21] D. A. V. Kliner and R. N. Zare, J. Chem. Phys. **92**, 2107 (1990).
[22] D. A. V. Kliner, K.-D. Rinnen, and R. N. Zare, Chem. Phys. Lett. **166**, 107 (1990).
[23] D. A. V. Kliner, D. E. Adelman, and R. N. Zare, J. Chem. Phys. **94**, 1069 (1991).
[24] H. Buchenau, J. P. Toennies, J. Arnold, and J. Wolfrum, Ber. Bunsenges. Phys. Chem. **94**, 1231 (1990), and references therein.
[25] M. A. Buntine, D. P. Baldwin, R. N. Zare, and D. W. Chandler, J. Chem. Phys. **94**, 4672 (1991).
[26] K.-D. Rinnen, D. A. V. Kliner, R. N. Zare, and W. M. Huo, Isr. J. Chem. **29**, 369 (1989); K.-D. Rinnen, M. A. Buntine, D. A. V. Kliner, R. N.

Zare, and W. M. Huo, J. Chem. Phys. **95**, 214 (1991).
[27] A. J. C. Varandas, F. B. Brown, C. A. Mead, D. G. Truhlar, and N. C. Blais, J. Chem. Phys. **86**, 6258 (1987).
[28] K.-D. Rinnen, D. A. V. Kliner, R. S. Blake, and R. N. Zare, Chem. Phys. Lett. **153**, 371 (1988).
[29] The BBO crystals were supplied by R. S. Feigelson and R. K. Route and grown as part of a research program sponsored in part by the Army Research Office, Contract No. DAAL03-86-K-0129, and in part by the NSF/MRL Program through the Center for Materials Research, Stanford University.
[30] K.-D. Rinnen, D. A. V. Kliner, R. S. Blake, and R. N. Zare, Rev. Sci. Instrum. **60**, 717 (1989).
[31] R. D. Levine and R. B. Bernstein, *Molecular Reaction Dynamics and Chemical Reactivity* (Oxford University, New York, 1987); I. M. W. Smith, *Kinetics and Dynamics of Elementary Gas Reactions* (Butterworths, London, 1980).
[32] W. J. van der Zande, R. Zhang, and R. N. Zare, in *Spectral Line Shapes*, edited by L. Frommhold and J. W. Keto (American Institute of Physics, New York, 1990), Vol. 6, p. 301; W. J. van der Zande, R. Zhang, R. N. Zare, K. J. McKendrick, and J. J. Valentini, J. Phys. Chem. (in press).
[33] R. D. Clear, S. J. Riley, and K. R. Wilson, J. Chem. Phys. **63**, 1340 (1975); R. Schmiedl, H. Dugan, W. Meier, and K. H. Welge, Z. Phys. A **304**, 137 (1982).
[34] D. A. V. Kliner, K.-D. Rinnen, and R. N. Zare, J. Chem. Phys. **90**, 4625 (1989); D. A. V. Kliner, K.-D. Rinnen, M. A. Buntine, D. E. Adelman, and R. N. Zare, *ibid.* **95**, 1663 (1991).
[35] K. P. Huber and G. Herzberg, *Molecular Spectra and Molecular Structure IV. Constants of Diatomic Molecules* (Van Nostrand Reinhold, New York, 1979).
[36] J. E. Pollard, D. J. Trevor, Y. T. Lee, and D. A. Shirley, J. Chem. Phys. **77**, 4818 (1982).
[37] D. R. Miller, in *Atomic and Molecular Beam Methods*, edited by G. Scoles (Oxford University, New York, 1988).
[38] J. P. Toennies and K. Winkelmann, J. Chem. Phys. **66**, 3965 (1977); G. Brusdeylins, H.-D. Meyer, J. P. Toennies, and K. Winkelmann, in *Rarefied Gas Dynamics. Proceedings of the 10th International Symposium*, edited by J. L. Potter, Part II, Vol. 5 of *Progress in Astronautics and Aeronautics* (AIAA, New York, 1977).
[39] R. Magnotta, D. J. Nesbitt, and S. R. Leone, Chem. Phys. Lett. **83**, 21 (1981).
[40] Z. Xu, B. Koplitz, and C. Wittig, J. Phys. Chem. **92**, 5518 (1988).
[41] C. A. Taatjes and S. R. Leone (private communication).
[42] I. Levy and M. Shapiro, J. Chem. Phys. **89**, 2900 (1988).
[43] C. E. Moore, Atomic Energy Levels, Vol. 1, U.S. Natl. Bur. Stand. Circ. 467, 1971.
[44] P. M. Aker, G. J. Germann, and J. J. Valentini, J. Chem. Phys. **90**, 4795 (1989).
[45] C. A. Boonenberg and H. R Mayne, Chem. Phys. Lett. **108**, 67 (1984); F. J. Aoiz, V. Candela, V. J. Herrero, and V. Sáez Rábanos, *ibid.* **169**, 243 (1990).
[46] I. Schechter, R. Kosloff, and R. D. Levine, Chem. Phys. Lett. **121**, 297 (1985).
[47] N. C. Blais and D. G. Truhlar, J. Chem. Phys. **88**, 5457 (1988).
[48] N. C. Blais and D. G. Truhlar, Chem. Phys. Lett. **162**, 503 (1989).
[49] C. W. Bauschlicher, Jr., S. R. Langhoff, and H. Partridge, Chem. Phys. Lett. **170**, 345 (1990).
[50] B. Lepetit and A. Kuppermann, Chem. Phys. Lett. **166**, 581 (1990).